Synthesis, Structures, and Properties of Side-Chain Cholesteric Liquid-Crystalline Polysiloxanes

Jian-She Hu, Bao-Yan Zhang, Lu-Mei Liu, Fan-Bao Meng

The Center for Molecular Science and Engineering, Northeastern University, Shenyang 110004, China

Received 25 November 2002; accepted 22 January 2003

ABSTRACT: The synthesis of three cholesteric monomers and side-chain liquid-crystalline polymers was described. The structure–property relationships of monomers IM–IIIM and polymers IP–IIIP were discussed. Their phase behavior and optical properties were investigated by differential scanning calorimetry, thermogravimetric analyses (TGA), and polarizing optical microscopy. Monomers IM–IIIM exhibited cholesteric oily-streak texture and focal-conic texture. Polymers IIP and IIIP revealed smectic A fan-shaped texture and cholesteric grandjean texture, respectively. Experimental results demonstrated that the selective reflection of IM–IIIM shifted to the short-wavelength region with increasing the flexible spacer length or decreasing the rigidity of the mesogen. Polymers with a longer flexible spacer had lower glass-transition temperatures and wider mesomorphic temperature ranges. TGA showed that the temperatures at which 5% weight loss occurred were greater than 300°C for all the polymers. © 2003 Wiley Periodicals, Inc. J Appl Polym Sci 89: 3944–3950, 2003

Key words: cholesteric phase; structure–property relations; liquid–crystalline polymers (LCP); glass transition; phase behavior

INTRODUCTION

Considerable interest has centered on thermotropic cholesteric liquid-crystalline polymers (ChLCPs) because of their outstanding optical properties such as selective reflection of light, thermochromism and circular dichroism, and potential applications such as flat-panel displays, full-color thermal imaging, and organic pigments.[1–9] The phase behavior and optical properties of side-chain ChLCPs mainly depend on the nature of the polymer backbone, the rigidity of the mesogen, and the flexible spacer length.[11–13] The polymer backbones of side-chain ChLCPs are primarily polyacrylates, polymethacrylates, and polysiloxanes. However, polyacrylates and polymethacrylates show higher glass-transition temperatures and higher viscosity because of their backbones. To obtain mesomorphic properties at moderate temperature, the polysiloxane backbone and a flexible spacer are usually used. The polymer backbone and the mesogenic units have antagonistic tendencies: the polymer backbone is driven toward a random coil–type configuration, whereas the mesogenic units stabilize with long-range orientation order. The mesogens are usually attached to the polymer backbone by a flexible spacer. The flexible spacer decouples the mesogenic side groups from the polymer backbone and renders the mesogens to order.

Recently, many novel side-chain cholesteric liquid-crystalline materials have been reported to explore their application.[14–17] The purpose of our research is (i) to study the structure–property relationships of side-chain ChLCPs, (ii) to supply necessary data to design and synthesize ChLCP networks, and (iii) to explore their applications in the fields of optical switches, color filters, and organic lacquers. In this study, the synthesis of side-chain cholesteric liquid-crystalline polysiloxanes is presented. Their phase behavior and optical properties were characterized by differential scanning calorimetry (DSC), thermogravimetric analyses (TGA), and polarizing optical microscopy (POM). The effects of the polymer backbone, the rigidity of the mesogen, and the flexible spacer length on phase behavior and optical properties are discussed in detail.

EXPERIMENTAL

Materials

Polymethylhydrosiloxane (PMHS, M_n = 700–800) was purchased from Jilin Chemical Industry Co. (China). Undecylenic acid was purchased from Beijing Jinlong Chemical Reagent Co., Ltd. (China). Cholesterol was purchased from Henan Xiayi Medical Co. (China). 4-Hydroxybenzoic acid was purchased from Beijing

Correspondence to: B.-Y. Zhang (baoyanzhang@hotmail.com).

Contract grant sponsor: National Natural Science Fundamental Committee of China.

Contract grant sponsor: National Basic Research Priorities Programme (973) of China.

Journal of Applied Polymer Science, Vol. 89, 3944–3950 (2003)

Fuxing Chemical Industry Co. (China). Toluene used in the hydrosilication reaction was first refluxed over sodium and then distilled. All other solvents and reagents were purified by standard methods.

Techniques

FTIR spectra were measured on a Nicolet 510 FTIR spectrometer (Nicolet Instruments, Madison, WI). Polymer sample films used for measurements were obtained by casting on a KBr table. Phase-transition temperatures and thermodynamic parameters were determined by using a TA Q100 DSC (TA Instruments, New Castle, DE) equipped with a liquid nitrogen cooling system. The heating and cooling rates were 20°C/min. The reported phase-transition temperatures were collected during the second-heating and the first-cooling scans. The thermal stability of the polymers under atmosphere was measured with a TA Q50 TGA thermogravimetric analyzer using a 20°C/min heating rate. A Leitz Microphot-FX (Leitz, Wetzlar, Germany) polarizing optical microscope equipped with a Mettler FP 82 hot stage and a FP 80 central processor were used to observe the phase-transition temperatures and to analyze mesomorphic properties for the liquid-crystalline monomers and polymers through observations of the optical textures.

Synthesis of the monomers

The synthesis of vinyl monomers was performed as shown in **Scheme 1.** Cholesteryl acrylate and cholesteryl undecylenate were prepared according to the literature procedures.[18]

4-(10-undecen-1-yloyloxy)benzoic acid

4-Hydroxybenzoic acid (34.5 g, 0.25 mol) was dissolved in 150 mL of tetrahydrofuran (THF) and 16 mL of pyridine. Undecyloyl chloride (40.5 g, 0.2 mol) was added dropwise to the above mixture at 5–10°C. After refluxing for 6 h, the reaction mixture was then poured into a large quantity of water, precipitated, filtered, and washed with water. The crude product was purified by recrystallization from ethanol. White crystals were obtained (mp = 128°C, yield = 58%).

IR (KBr, cm^{-1}): 3080 (═C—H); 2925, 2852 (–CH_2–); 2672, 2557 (–COOH); 1754, 1684 (C═O); 1641 (C═C); 1602, 1508 (Ar–).

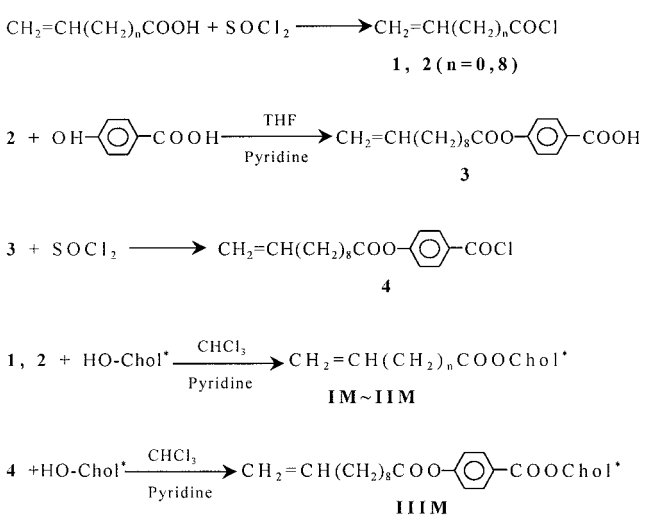

Scheme 1 Synthetic routes of monomers.

4-(10-undecen-1-yloyloxy)benzoyl chloride

4-Undecyloyloxybenzoic acid (30.4 g, 0.1 mol) was reacted at 50°C with 30 mL of thionyl chloride containing a few drops of *N,N*-dimethylformamide for 5 h, and then the excess thionyl chloride was removed under reduced pressure to give the corresponding acid chloride. Yield = 92%.

Cholesteryl-4-10-undecen-1-yloyloxy)benzoate

In a 100-mL three-neck flask, cholesterol (15.5 g, 0.04 mol) and 3.2 mL of pyridine were dissolved in 100 mL of chloroform. Then, 4-undecyloyloxybenzoyl chloride (12.9 g, 0.04 mol) in 20 mL of chloroform was added dropwise at 10–15°C. The reaction mixture was stirred at room temperature for 10 h. The precipitate was removed by filtration, and the crude product was precipitated by adding ethanol to the filtrate and recrystallized from toluene.

IR (KBr, cm^{-1}): 2930, 2852 (CH_3–, –CH_2–); 1767, 1716 (C═O); 1635 (C═C); 1603, 1504 (Ar).

Synthesis of the polymers

The synthetic routes of the polymers are outlined in **Scheme 2.** All synthesized polymers are listed in Table I. Polymers IP–IIIP were prepared by the same method. The synthesis of IIIP is described below.

The monomers IIIM and PMHS were dissolved in dry, freshly distilled toluene. The reaction mixture was heated to 60°C under nitrogen and anhydrous conditions, and then a proper amount of THF solution of hexchloroplatinate (IV) hydrate catalyst was injected with a syringe. The reaction was maintained for 24 h. The solvent was removed, and the crude polymers were purified by repeated precipitation in toluene with excess methanol and then dried under vacuum.

IR (KBr, cm^{-1}): 2933, 2856 (CH_3–, –CH_2–); 1765, 1717 (C═O); 1605, 1505 (Ar–); 1272 (Si—C); 1000–1200 (Si—O—Si).

RESULTS AND DISCUSSION

Synthesis

The synthetic routes for the target monomers and polymers are shown in **Schemes 1** and **2**. 4-(10-Unde-

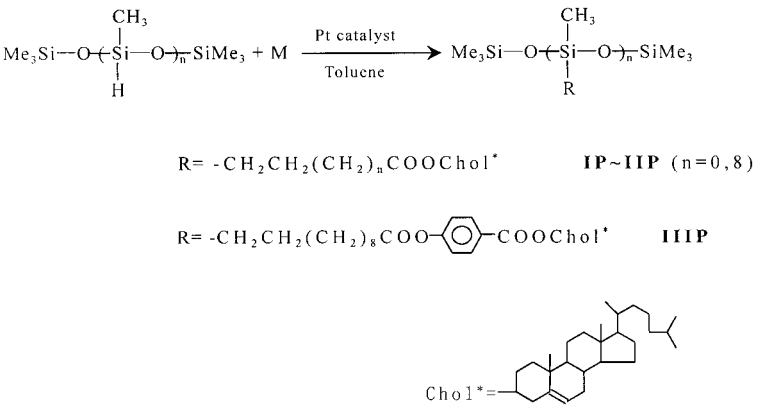

Scheme 2 Synthetic routes of polysiloxanes.

cen-1-yloyloxy)benzoic acid **3** was prepared by reacting undecyloyl chloride **2** with 4-hydroxybenzoic acid in the presence of pyridine in THF. Then, 4-(10-undecen-1-yloyloxy)benzoyl chloride **4** was obtained by acylation reaction. Finally, **1, 2**, and **4** were reacted with cholesterol in the presence of pyridine in chloroform to obtain the vinyl monomers. FTIR spectra of the monomers showed characteristic bands at around 1760 and 1710 cm^{-1} attributed to ester C═O stretching, around 1635 cm^{-1} attributed to vinyl C═C stretching, and around 1603 and 1504 cm^{-1}, corresponding to aromatic C═C stretching.

Polymerization was carried out by a hydrosilication reaction between the Si—H groups of PMHS and the double bonds (C═C) of the mesogenic side groups in toluene, using hexchloroplatinate (IV) hydrate as catalyst at 60°C. Details of the polymerization reaction are represented in Table I. All the polymers were soluble in hydrocarbons (e.g., toluene, xylene), but were insoluble in hydroxy-group–containing solvents such as methanol and ethanol. FTIR spectra of the polymers showed the complete disappearance of the Si—H stretching band at 2160 cm^{-1} and the vinyl C═C stretching band at 1635 cm^{-1}. Their characteristic absorption bands appeared at 1760–1715, 1605 and 1502, 1270, and 1200–1000 cm^{-1}, corresponding to the stretching of ester C═O, aromatic, Si—C, and Si—O—Si, respectively.

Optical properties

The unique optical properties of side-chain ChLCPs are related to the helical supermolecular structure of the cholesteric phase, the helical pitch of which controls the wavelength of the selectively reflected light, and the reflection color can be observed if the pitch length is consistent with the wavelength of visible light. For side-chain ChLCPs, the pitch mainly depends on the polymeric structure such as the polymer backbone, rigidity of the mesogen, the flexible spacer length, the copolymer composition, molecular mass, and outer condition, for example, temperature, force field (e.g., shearing), electric field, and magnetic field. According to the Bragg equation: $\lambda_m = np \cos \phi$, the wavelength of the reflected light λ_m is related to the pitch p, the average refractive n, and the observation angle ϕ. Therefore, the pitch affects not only the reflection color, but also the optical textures of the cholesteric phase. When the pitch lies within the visible light, the cholesteric phase exhibits planar oily-streak or grandjean texture; when the pitch is much greater than the wavelength of visible light, the fingerprint texture can be observed; when the pitch is less than the wavelength of visible light, the focal-conic texture is observed. However, the focal-conic texture can easily change into oily-streak or grandjean texture by slight shearing. However, the fingerprint texture cannot

TABLE I
Polymerization and Thermal Properties of the Polymers

Polymer	n	Feed (mmol) PMHS	Feed (mmol) M	Yield (%)	T_g (°C)	T_i (°C)	ΔH (J/g)	ΔT[a] (°C)	T_d[b] (°C)
IP	0	1	7	88	84.2	—	—	—	328.6
IIP	8	1	7	90	23.7	153.6	2.61	129.9	322.4
IIIP	—	1	7	93	38.6	233.6	1.73	195.0	316.2

[a] Mesomorphic temperature ranges.
[b] Temperature at which 5% weight loss occurred.

change into planar oily-streak or grandjean texture. In addition, the planar texture and focal-conic texture can also transform each other by electric field and magnetic field.

The texture and main reflection color of the monomers and polymers observed by POM under nitrogen atmosphere are shown in Table II. As can be seen from Table II, the polymer backbone, the rigidity of the mesogen, and the flexible spacer length strongly influenced the pitch and the reflection color of the cholesteric phase. For IM–IIIM, the pitch decreased and the selective reflection of light shifted to the short-wavelength region (blue shift) with increasing the flexible spacer length or decreasing the rigidity of the mesogen. For IP–IIIP, IP did not reveal any mesomorphic behavior because of the shorter spacer length and greater steric hindrance of the bulky cholesteryl group, which disturbed the orientation of the mesogen. IIP displayed a smectic A phase according to the literature,[18] but can change into the cholesteric phase by the copolymerization of IIM and other monomer (such as nematic, smectic, chiral, etc.).[18,19] IIIP revealed a cholesteric phase, and no reflection color was observed, but a different reflection color can be seen by changing the copolymer composition.[20]

POM observations showed that the monomers IM–IIIM, in turn, exhibited enantiotropic oily-streak texture and focal-conic texture of the cholesteric phase during the heating and cooling cycles. When these monomers were heated to the melting temperature, the obvious oily-streak texture appeared, and the reflection color was observed. By cooling the samples from the isotropic melt, the focal-conic texture was formed, which easily transformed to oily-steak texture by shearing the mesomorphic phase. Photomicrographs of IM are shown in Figure 1(a), (b). Polymer IIP exhibited smectic fan-shaped texture, and IIIP displayed cholesteric grandjean texture. A photomicrograph of IIIP is shown in Figure 2.

Thermal properties

The thermal properties of the monomers and polymers were determined by DSC and POM. Both the second-heating and the first-cooling cycles were recorded. The phase-transition temperatures and corresponding enthalpy changes are listed in Tables I, II, and III, respectively. All phase transitions were reversible on repeated heating and cooling cycles. Thermal properties determined by DSC were consistent with POM observation results. Typical DSC curves of IM–IIIM and IP–IIIP are shown in Figures 3 and 4, respectively.

DSC heating curves of IM–IIIM showed two endotherm peaks, which represented, respectively, a melting transition and a cholesteric to isotropic phase transition. On the cooling scan of IM and IIIM, two exotherm peaks revealed an isotropic to cholesteric phase transition and crystallization transition. However, on the cooling scan of IIM, an isotropic to cholesteric phase, cholesteric to smectic phase, and crystallization transition appeared at 84.2, 68.8, and 41.9°C, respectively. As can be seen from the data listed in Tables I and III, the phase behavior of IM–IIIM was strongly influenced by the rigidity of the mesogen and the flexible spacer length. Compared with the melting temperature (T_m) and the isotropization temperature (T_i) of IM, T_m and T_i of IIM decreased by 0.6 and 38.7°C, respectively. Because T_i decreased more than T_m, the mesomorphic temperature ranges (ΔT) narrowed to 38.1°C. For IIM and IIIM, the T_m and T_i of IIIM increased by 31.0 and 109.9°C, respectively, compared to those of IIM; because T_i increased more than T_m, ΔT widened to 78.9°C. The above phenomena are explained as follows: (1) When the spacer length increases, the molecular flexibility also increases, which causes a decrease in T_m and T_i; (2) when the rigidity of the mesogen increases, the intermolecular arrange-

TABLE II
POM Data of the Monomers and Polymers

Sample	n	T_m (°C)	T_t[a] (°C)	T_{a1}[b] (°C)	T_c[c] (°C)	Texture	Main reflected color
IM	0	78	127	125	58	Oily streak Focal-conic	blue
IIM	8	80	89	83	54	Oily streak Focal-conic	violet
IIIM	—	104	202	201	82	Oily streak Focal-conic	green
IP	0	—	—	—	—	—	—
IIP	8	—	155	151	—	Fan-shaped	—
IIIP	—	—	241	232	—	Grandjean	—

[a] Temperature at which the birefringence disappeared completely.
[b] Temperature at which the mesomorphic phase occurred.
[a] Temperature at which the crystallization occurred.

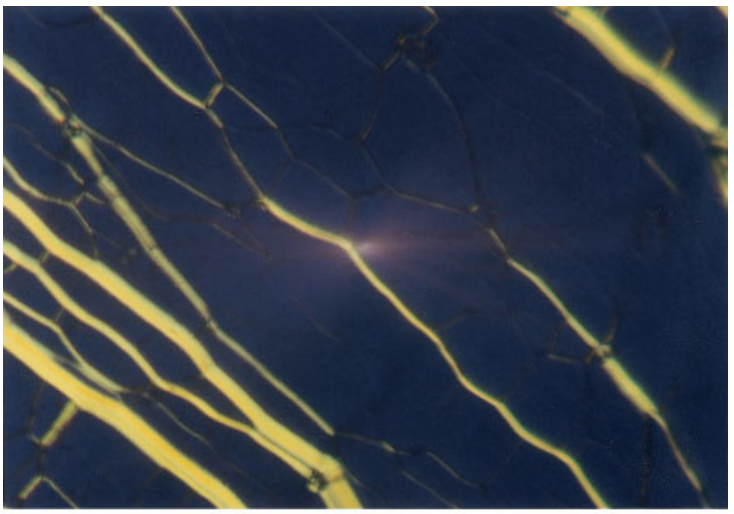

(a)

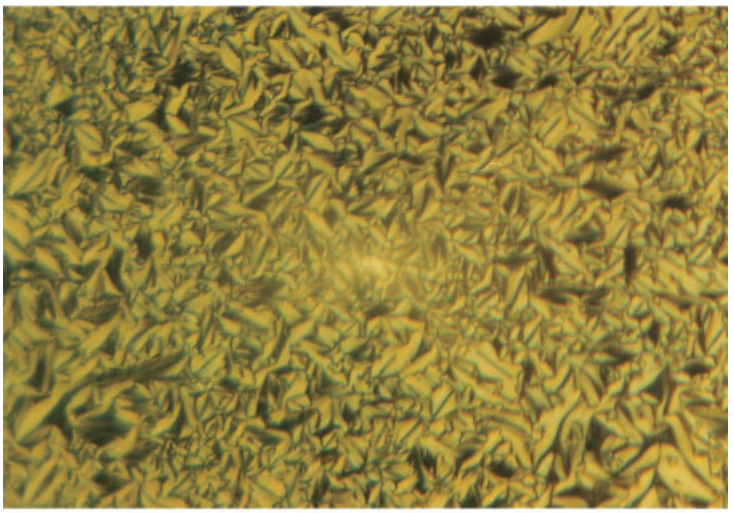

(b)

Figure 1 POM micrographs of IM (×200): (a) oily-streak texture observed at 88°C; (b) focal-conic texture observed at 115°C.

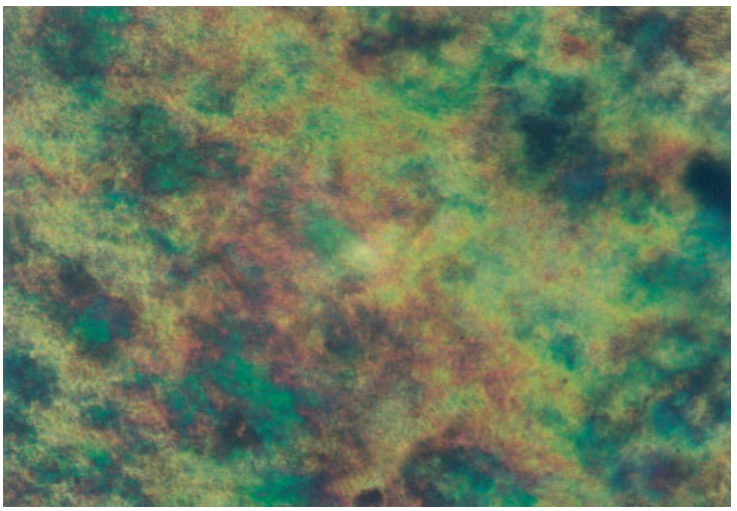

Figure 2 POM micrographs of IIIP (×200): grandjean texture observed at 183°C.

TABLE III
Phase-Transition Temperatures of the Monomers

Monomer	n	Phase-transition temperature[a] in °C (corresponding enthalpy changes in J/g) Heating / Cooling	Yield (%)	ΔT[b] (°C)
IM	0	K79.6(48.82)Ch124.3(1.25)I / I119.1(0.93)Ch25.5(10.29)K	62	44.7
IIM	8	K79.0(63.08)Ch85.6(0.41)I / 184.2(1.08)Ch68.8(0.91)S_A41.9(48.13)K	65	6.6
IIIM	—	K110.0(20.64)Ch195.5(1.82)I / 1185.5(0.54)Ch69.4(19.16)K	46	85.5

[a] Peak temperatures were taken as the phase-transition temperatures. K, solid; N, nematic; Ch, cholesteric; S, smectic; I, isotropic.
[b] Mesomorphic temperature ranges.

ment draws closer and the intermolecular force is enhanced, which causes an increase in T_m and T_i.

On the heating scan of IIP and IIIP, a glass transition and a cholesteric to isotropic phase transition were observed. However, the DSC curve of IP showed only a glass transition and no mesomorphic to isotropic phase transition, which agreed with POM observation results. According to the data listed in Table I, the spacer length and the rigidity of the mesogen also had a profound effect on the phase transition and mesomorphic properties of the obtained polymers. For IIP and IIIP, when the rigidity of the mesogen increased, the glass-transition temperature (T_g) and the T_i increased, although T_g increased less than T_i. This result suggests that a larger rigid mesogen can lead to a wider mesomorphic temperature range, thus tending to stabilize the mesomorphic phase.

For side-chain ChLCPs, the T_g value is affected by the polymer backbone, the mesogen, and the flexible spacer length. For IP and IIP, with an increase of the spacer length, the flexibility of the polymer chain also increases, which increases the motion of chain segments, so the T_g value decreases. For IIP and IIIP, with increasing the rigidity of the mesogen, the motion of chain segments decreases, which causes an increase in the T_g value. As can be seen in Table I, an increase of the spacer length of IP and IIP from $n = 0$ to $n = 8$ caused a decrease in the T_g value of 60.5°C. In addition, an increase of the rigidity of the mesogen caused an increase in the T_g value of 14.9°C.

The mesomorphic temperature ranges of IIP and IIIP were much greater than those of the corresponding monomers IIM and IIIM, which indicated that polymerization can result in the stabilization of the mesomorphic phase. TGA indicated that the temperatures at which 5% weight loss occurred were greater than 300°C for IP–IIIP, which showed that the synthesized side-chain cholesteric liquid-crystalline polysiloxanes had higher thermal stability.

In a comparison of the phase-transition temperatures of IP–IIIP, a flexible polymer backbone, longer flexible spacer, and larger rigid mesogenic core can be seen here to have a tendency toward exhibiting lower glass-transition temperatures and a wide range of mesomorphic temperatures.

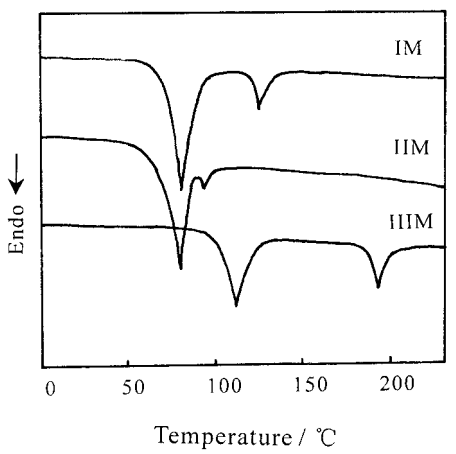

Figure 3 DSC thermograms of the monomers IM–IIIM.

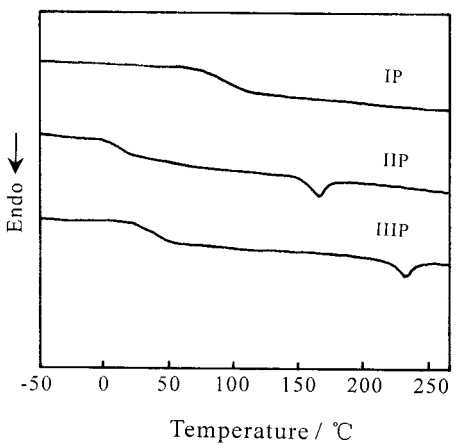

Figure 4 DSC thermograms of the polymers IP–IIIP.

CONCLUSIONS

We successfully synthesized three cholesteric monomers and their corresponding polymers. Monomers IM–IIIM exhibited cholesteric oily-streak texture and focal-conic texture. Polymers IIP and IIIP revealed smectic A phase and cholesteric phase, respectively. All phase transitions were reversible on repeated heating and cooling cycles. The selective reflection of IM–IIIM shifted to the short-wavelength region with increasing the flexible spacer length or decreasing the rigidity of the mesogen. In polymers IP–IIIP, a longer flexible spacer tended to exhibit lower glass-transition temperatures, and a larger rigid mesogenic core could lead to higher isotropization temperature and a wider range of mesomorphic temperatures.

The authors are grateful to the National Natural Science Fundamental Committee of China and the National Basic Research Priorities Programme (973) of China for financial support of this work.

References

1. Jacobs, S. D. J Opt Soc Am 1988, B5, 1962.
2. Belayev, S. V.; Schadt, M. I.; Funfschiling, J.; Malimoneko, N. V.; Schmitt, K. Jpn J Appl Phys 1990, 29, L634.
3. Broer, D. J.; Lub, J.; Mol, G. N. Nature 1995, 378, 467.
4. Bunning, T. J.; Kreuzer, F. H. Trends Polym Sci 1995, 3, 318.
5. Yang, D. K.; West, J. L.; Chien, L. C.; Doane, J. W. J Appl Phys 1994, 76, 1331.
6. Kricheldorf, H. R.; Sun, S. J.; Chen, C. P.; Chang, T. C. J Polym Sci Part A: Polym Chem 1997, 35, 1611.
7. Peter, P. M. Nature 1998, 391, 745.
8. Sapich, B.; Stumpe, J.; Krawinkel, T.; Kricheldorf, H. R. Macromolecules 1998, 31, 1016.
9. Sun, S. J.; Liao, L. C.; Chang, T. C. J Polym Sci Part A: Polym Chem 2000, 38, 1852.
10. Le Barney, P.; Dubois, J. C.; Friedrich, C.; Noel, C. Polym Bull 1986, 15, 341.
11. Hsu, C. S.; Percec, V. J Polym Sci Part A: Polym Chem 1989, 27, 453.
12. Hsiech, C. J.; Wu, S. H.; Hsiue, G. H.; Hsu, C. S. J Polym Sci Part A: Polym Chem 1994, 32, 1077.
13. Wu, Y. H.; Lu, Y. H.; Hsu, C. S. J Macromol Sci Pure Appl Chem 1995, A32, 1471.
14. Stohr, A.; Strohriegl, P. Macromol Chem Phys 1998, 199, 751.
15. Dierking, I.; Kosbar, L. L.; Held, G. A. Liq Cryst 1998, 24, 387.
16. Pfeuffer, T.; Strohriegl, P. Macromol Chem Phys 1999, 200, 2480.
17. Espinosa, M. A.; Cadiz, V.; Galia, M. J Polym Sci Part A: Polym Chem 2001, 39, 2847.
18. Hu, J. S.; Zhang, B. Y.; Zang, B. L. J Appl Polym Sci 2002, 86, 2670.
19. Zhi, J. G.; Zhang B. Y.; Zang, B. L.; Shi, G. H. J Appl Polym Sci 2002, 85, 2115.
20. Zhang, B. Y.; Hu, J. S. Macromol Chem Phys, to appear.